Biophysical Journal Volume 65 October 1993 1363–1370

The Effect of a Variable Dielectric Coefficient and Finite Ion Size on Poisson-Boltzmann Calculations of DNA-Electrolyte Systems

George R. Pack, G. A. Garrett, Linda Wong, and Gene Lamm
Department of Biomedical Sciences, University of Illinois College of Medicine at Rockford, Rockford, Illinois, USA

ABSTRACT The results of variable dielectric coefficient Poisson-Boltzmann calculations of the counter-ion concentration in the vicinity of an all-atom model of the B-form of DNA are presented with an emphasis on the importance of spatial variations in the dielectric properties of the solvent, particularly at the macro-ion–solvent interface. Calculations of the distribution of hard-sphere electrolyte ions of various dimensions are reported.

The presence of a dielectric boundary significantly increases the magnitude of the electrostatic potential with a concomitant increase in the accumulation of small counter-ions in the groove regions of DNA. Because ions with radii greater than 2 Å have restricted access to the minor groove, the effect there is less significant than it is within the major groove. Changes in the dielectric coefficient for the electrolyte solution, allowing variation from 10 to 25, 40, 60, and 78.5 within the first 7.4 Å of the surface of DNA, substantially increases the calculated surface concentration of counter-ions of all sizes. A lower dielectric coefficient near the macro-ion surface also tends to increase the counter-ion density in regions where the electrostatic potential is more negative than $-kT$. Regardless of the choice of dielectric coefficient, the number of ions in regions where the electrostatic potential is less than $-kT$ remains the same for 0.153 M added 1-1 monovalent electrolyte as for the case without added salt.

The strong dependence of the calculated distribution of counter-ion density on the choice of dielectric coefficients representing the solvent continuum suggests that care must be taken to properly characterize the physical system when studying electrostatic properties using these methods.

INTRODUCTION

In previous work (Pack et al., 1990), comparison of the results of Poisson-Boltzmann (PB) calculations with those obtained by Metropolis Monte Carlo calculations on identical all-atom models of DNA in an dielectric continuum containing 1-1 added monovalent salt indicated that the errors in PB are greatest in those regions where the counter-ion density is greatest—within the grooves of DNA. Since the previous calculations invoked the approximation of a uniform dielectric coefficient for the entire DNA-electrolyte system and since the presence of a dielectric boundary has been shown to focus the electric field in macromolecular crevices (Klapper et al., 1986), the present study was undertaken to determine the extent to which a dielectric boundary affects the accumulation of hard-sphere electrolyte ions in the grooves of DNA.

The study of the electrostatic properties of macro-ions, particularly of proteins, has been advanced by the development of techniques for solving the PB equation in the presence of a dielectric boundary. Warwicker and Watson (1982) introduced a method for solving the three-dimensional Poisson equation for a protein-water system, and Warwicker (1986) later extended this technique to include electrolyte ions in a linearized Boltzmann approximation. Numerous groups (Gilson et al., 1985; Zauhar and Morgan, 1985; Rogers et al., 1985; Warwicker et al., 1985) have contributed to the concept that a macromolecule with a low dielectric coefficient, immersed in a medium of high dielectric coefficient, will have regions of enhanced potential within its surface clefts. Jayaram et al. (1989) presented a Cartesian grid-based solution to the nonlinear Poisson-Boltzmann equation for DNA with an electrolyte environment and found significant effects caused by the dielectric boundary. This local modification of the electrostatic potential within these clefts is particularly sensitive to the shape of the dielectric boundary. To circumvent the inaccurate description of the molecular surface by a grid of cubic finite elements, recent approaches have introduced a "dielectric boundary smoothing" (Davis and McCammon, 1991) and a finite element algorithm that allows the use of noncubic grids (You and Harvey, 1992). A recent application of the numerical solution of the PB equation to calculate the electrostatic forces exerted by a high dielectric aqueous solvent on the solute surface (Gilson et al. 1993) finds a substantial contribution of the boundary effect on these forces. The present paper presents an investigation of the dielectric boundary effect using a non-Cartesian grid coupled with counter-ions of finite size and local variations in the dielectric properties of the solvent continuum.

These dielectric boundary methods (Warwicker and Watson, 1982; Warwicker, 1986; Gilson et al., 1985; Zauhar and Morgan, 1985; Rogers et al., 1985; Warwicker et al., 1985; Jayaram et al., 1989) have been revised to take advantage of the non-Cartesian grid techniques developed in our laboratory (Klein and Pack, 1983; Pack and Klein, 1984; Pack et al., 1986a,b; Lamm and Pack, 1990) to yield a method for solving the full PB equation in the presence of a precisely defined dielectric boundary and finite, hard-sphere counter-ions. In

Received for publication 21 October 1992 and in final form 14 July 1993.
Address reprint requests to Dr. George R. Pack, Department of Biomedical Sciences, University of Illinois College of Medicine at Rockford, 1601 Parkview Avenue, Rockford, IL 61107.

0006-3495/93/10/1363/08 $2.00

addition to issues relating to the accuracy of the algorithm, this paper also addresses the effect of a variable dielectric coefficient on the focusing of the electric field in the grooves of the helical duplex.

MATERIALS AND METHODS

The atomic positions and charges for the B-form of poly(dG)·poly(dC) are the same as those used in previous calculations (Klein and Pack, 1983; Pack and Klein, 1984; Pack et al., 1986a,b; Lamm and Pack, 1990). A nucleotide pair with a net charge of two electrons serves as a periodic unit, neutralized by a 1-1 monovalent electrolyte with an excess of two cationic charges in its environment. Periodic conditions assume identical electrolyte ion distributions around identical nucleotide pairs translated by 3.38 Å up and down the helical axis and rotated by $\pi/5$ and $-\pi/5$ radians about that axis. The full system was assumed to extend infinitely along the helical axis.

The electrolyte ions were restricted to a cell extending 45 Å radially from the helical axis. Confining the system to a 45 Å cylinder corresponds to a phosphate concentration of 0.153 M and a nucleic acid density of 90.9 g/liter. The hard-sphere electrolyte ions do not have access to the space occupied by the DNA. The normalization condition for the electrolyte, discussed below, extends over the volume to which the ions have access, with larger ions having access to slightly less volume. For the case without added salt, counter-ions appear to be present at a higher concentration than the phosphate groups that they neutralize since the electrolyte is presumed to have access to less volume. For the system without added salt, the neutralizing concentrations of ions are 0.164 M for ions with a 1-Å radius, 0.167 M for 2-Å ions, and 0.173 M for 4-Å ions. For the calculations with added salt, the concentrations used were 0.317 M counter-ion with 0.153 M co-ion for the 1-Å case, 0.323 M counter-ion with 0.156 M co-ion for the 2-Å case, and 0.334 M counter-ion with 0.161 M co-ion for the 4-Å case.

Aside from the normalization condition and the finite size of electrolyte ions, the present work differs from the PB dielectric boundary calculations of others in the use of a non-Cartesian grid (shroud) that is contoured to the surface of the macro-ion. This permits a precise, smooth representation of the macro-ion–environment boundary, dividing the volume of the system into the space occupied by the central ion and regions of its environment that are available to electrolyte ions of different sizes. The first step in the generation of the irregular environmental grid is the use of planar cross-sectional cuts through the macro-ion. Planar cuts are spaced 3.38 Å apart along the helical axis. Each cut yields a series of circles representing slices through the van der Waals' sphere for each macro-ion atom. The union of these circles provides the effective interaction surface of the macro-ion for point electrolyte ions. The black shaded area in Fig. 1 shows this projection for a cross-section perpendicular to the helical axis of the B conformation of poly(dG)·poly(dC). It might be noted that this does not define a single closed figure; in the plane defined in Fig. 1, there is a total of three areas that are two-dimensional projections of the volume that would be inaccessible to point particles.

Environmental regions inaccessible to hard-sphere ions of radius a are defined by the projections of spheres with radii equal to the sum of their van der Waals radii plus a: the first shroud layer in Fig. 1 (indicated by arrow 1) inaccessible to ions with radii 1 Å or larger, the second to ions with radii 2 Å or larger (arrow 2), and the third to ions with radii 4 Å or larger (arrow 3). This approach allows the use of a single shroud for all of the calculations presented here. The 1-Å, 2-Å, and 4-Å ions have access to different domains, each progressively smaller and more distant from the macro-ion surface. Note that the continuous boundary defining the accessible perimeter for the 1-Å ions (the outer boundary of layer 1) encompasses all three closed projections of the DNA atoms onto this plane. Additional outer layers to which all of the electrolyte ions have access are then defined out to a radial distance of 45 Å from the helical axis. This distance was chosen because of the relatively high DNA concentration (90.9 g/liter) used in in vitro experimental studies.

Each layer thus defined is subdivided into cells by placing points representing the approximate centers of the cells at regular intervals along a path passing through the center of the layer. For each of the five inner layers a geometric determination is made to set up the boundaries of cells of approximately equal volume. For the inner three layers, regions from which at least some ions are excluded, the curved surfaces of closest approach (as indicated in Fig. 1) are included as part of each cell boundary. For the fourth and fifth inner layers, polygons defined by the intersection of the perpendicular bisectors of line segments connecting all adjacent cells in the plane are used.

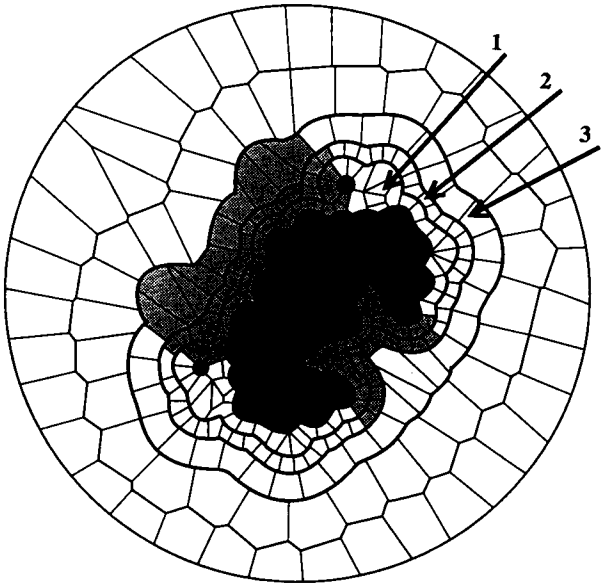

FIGURE 1 A gridded representation of DNA and environmental shroud 1; a cross-sectional view of the inner volume enclosed by a 21-Å cylinder centered at the helical axis of DNA. Area in black depicts the projections of the van der Waals spheres of the DNA atoms onto this plane. Arrows indicate layers 1, 2, and 3. Hard spheres with a 1-Å radius are excluded from layer 1; those with a 2-Å radius are excluded from layer 2; spheres with a 4-Å radius are excluded from layer 3. Shaded areas show the major and minor groove regions; the larger area represents the major groove.

Each cell extends for a fixed distance in the dimension parallel to the helical axis (*i.e.*, perpendicular to the plane of the paper in Fig. 1). The area of each cell as well as the area of overlap of adjacent cells is calculated from geometric relations that are exact. The volume of each cell is then calculated by multiplying the area by the interplanar distance. Thus the boundaries and volumes are exact in two dimensions and approximate in the axial direction.

The definition of a dielectric boundary requires a grid representation of the interior of DNA as well as of its external environment. A Cartesian grid is the most straightforward lattice to construct for that portion of the DNA that does not border the curved van der Waals surface (such a grid is presented in Fig. 2). The curved DNA boundary defined by the distance of closest approach of a point particle has been replaced by a series of straight line segments. The boundaries that define the distance of closest approach of the hard-sphere ions remain curved. Atomic charges of the macro-ion are mapped onto the grid in proportion to the overlap of the atom's van der Waals sphere with the grid elements. Fig. 2 depicts both the interior and exterior finite elements of one planar cut through that portion of the DNA-environment system enclosed by a 21-Å cylinder. The shaded areas represent the groove regions. Those shaded elements inside the innermost curved boundary are in a region that is inaccessible to 1-Å ions yet outside the van der Waals suface of the macro-ion.

In the work of Warwicker and Watson (1982), the electrostatic potential due to the charge distribution, $\rho(r)$, of a protein of arbitrary shape and with dielectric coefficient ϵ_p, was defined for the protein in a continuum of dielectric coefficient ϵ_s. No electrolyte ions were considered, although a uniform Cartesian grid was constructed in order to define $\epsilon(r)$ as either ϵ_p or ϵ_s. The essence of the calculation lies in the definition of the potential in cell i in terms of the potentials in the surrounding cells, as discussed by

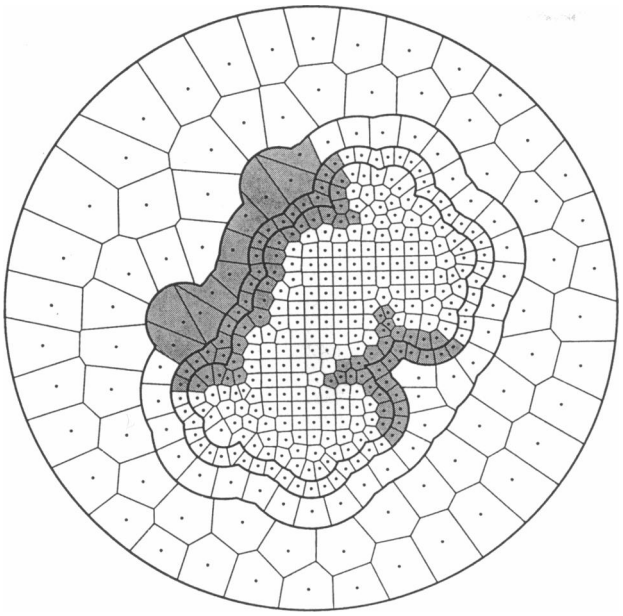

FIGURE 2 A representation of the non-Cartesian grid used in the calculations presented. The grid for the interior of DNA is included. Dots are in the centers of the finite volume elements. Shaded regions represent the major and minor groove projections. This corresponds to Fig. 1; DNA grid has been added.

Wachspress (1966). In that work, the Poisson equation

$$-\nabla\cdot[\epsilon(r)\nabla\phi(r)] = \rho(r)/\epsilon_o \tag{1}$$

was approximated by the finite element representation

$$\sum_j[(\phi_i - \phi_j)\,\epsilon_{ij}] = \rho_i h^2 \epsilon_o, \tag{2}$$

where ϵ_{ij} is the arithmetic average of the dielectric coefficients in elements i and j, with j varying over all volume elements bordering on element i, and h is the grid spacing.

Combining the contoured lattice of our previous work with the equations for a dielectric boundary and the Boltzmann equation for the charge density in the environment should provide a flexible method for the description of the ion atmosphere of DNA within the Poisson-Boltzmann approximation. The potential at point i in the system (i.e., inside the macro-ion or in the environment) is given by rearranging the analogue of Eq. 2 for an irregular grid:

$$\phi_i = \left[4\pi v_i\rho_i/\epsilon_o + \sum_j(\phi_j\epsilon_{ij}S_{ij}/r_{ij})\right] \Big/ \sum_j(\epsilon_{ij}S_{ij}/r_{ij}), \tag{3}$$

where v_i is the volume of element i, S_{ij} is the surface area shared by bordering elements i and j, $\epsilon_{ij} = (\epsilon_i + \epsilon_j)/2$, and r_{ij} is the distance between the centers of elements i and j. Index j ranges over all volume elements that border element i (i.e., for which S_{ij} is nonvanishing).

The dielectric coefficient of elements inside DNA was set to 2 (Klapper et al., 1986), while the external dielectric coefficient was varied from that of bulk water (78.5) to the lower values expected to be present at the macro-ion surface due to the high electric fields. The calculations consisted of the following steps:

1. An initial set of charge densities (ρ_i) and electrostatic potentials (ϕ_i) is obtained for all environmental volume elements based on the previous uniform dielectric coefficient method (Pack et al., 1990).
2. An updated set of electrostatic potentials is calculated for each volume element in the system (DNA and environment) using Eq. 3.
3. An updated set of environmental charge densities is calculated for each ion type from the normalized Boltzmann expression:

$$\rho_i^k = N_k \exp(-\beta z_k\phi_i) \Big/ \sum_j \nu_j \exp(-\beta z_k\phi_j), \tag{4}$$

where N_k is the number of ions of type k within the repeat unit, z_k is the charge of the type of ion considered (+1 or −1 for the monovalent ions considered here), and the sum over j includes only those elements in the repeat unit to which ion type k has access.

A convergence quantity, A, is defined as the sum of the counter-ion normalization coefficient (ion type 1) plus the total electrolyte charge in the first accessible layer,

$$A = \sum_j \nu_j \exp(-\beta z_1\phi_j) + \sum_k \rho_k\nu_k, \tag{5}$$

in which j again ranges over elements to which ion type 1 ($z_1 = 1$) has access and k ranges over the first accessible environment layer for ion type 1. Steps 2 and 3 are reiterated until the difference between successive values of A is less than 0.0001.

Some PB calculations were performed to explore the prediction of counter-ion condensation theory (Manning, 1978), that a constant number of cationic charges per phosphate group are "bound" to DNA regardless of the concentration of electrolyte in the environment. For these calculations a definition of binding was chosen in which ions in regions where the potential is more negative than $-kT$ are considered to be bound.

RESULTS

Several sets of Poisson-Boltzmann calculations were performed to determine the effect of different approximations on the distribution of electrolyte charge around the B form of DNA. Electrolyte ions were modeled as hard spheres of radii of 1, 2, and 4 Å in a dielectric continuum. Calculations were done for the DNA-environment system with a neutralizing number of monovalent counter-ions (no added salt) and with 0.153 M added 1-1 monovalent salt. Tables 1, 2, and 3 present the results for 1, 2, and 4 Å ions, respectively.

In order to test the accuracy of the algorithm, a set of calculations using the uniform dielectric algorithm (Klein and Pack, 1983; Lamm and Pack, 1990; Pack and Klein, 1984; Pack et al., 1986a,b, 1990) was performed for comparison. This method, utilizing a uniform dielectric coefficient, is designated as PB^0, and the results are tabulated in column A of Tables 1, 2, and 3. The PB^0 calculations differ from our earlier work (Pack et al., 1990) in that the atomic charges of DNA were mapped onto the interior DNA grid described above and the resulting point charges were used to calculate the electrostatic potential arising from DNA using Coulomb's law. In that work (Pack et al., 1990), it was seen that the greatest accumulation of counter-ion charge was in the groove regions. In the present calculations the accumulation is again greatest in the grooves, although there is some redistribution of counter-ion density that may be ascribed to different representations of the charge distribution of the polyion; the mapping of the charge distribution for a nucleotide pair from the atomic centers onto a single planar grid of finite elements is the only difference between these two calculations.

The dielectric boundary algorithm described in the previous section is designated PB^1. An initial set of calculations

TABLE 1 Concentration (mol/liter) of 1-Å hard sphere counter-ions in the helical grooves of DNA (0.153 M PO_4) by radial layer

		No added salt				0.153 M added salt		
R (Å)*		A	B	C	D	B	C	D
1.5	Major groove	4.10	4.38	4.85	8.33	4.85	5.33	8.78
	Minor groove	3.64	3.75	8.35	12.45	4.22	9.33	13.11
	Elsewhere	1.44	1.57	1.59	2.17	1.98	2.12	2.96
	Total	2.55	2.72	3.59	5.55	3.15	4.17	6.22
3.0	Major groove	2.17	1.98	1.73	2.18	2.21	1.98	2.49
	Minor groove	0.00	0.00	0.00	0.00	0.00	0.00	0.00
	Elsewhere	0.81	0.82	0.61	0.35	1.08	0.87	0.61
	Total	1.21	1.17	0.94	0.89	1.42	1.20	1.17
5.69	Major groove	0.00	0.00	0.00	0.00	0.00	0.00	0.00
	Minor groove	0.00	0.00	0.00	0.00	0.00	0.00	0.00
	Elsewhere	0.42	0.36	0.33	0.20	0.54	0.50	0.38
	Total	0.42	0.36	0.33	0.20	0.54	0.50	0.38
9.07	Major groove	0.00	0.00	0.00	0.00	0.00	0.00	0.00
	Minor groove	0.00	0.00	0.00	0.00	0.00	0.00	0.00
	Elsewhere	0.18	0.17	0.16	0.10	0.33	0.31	0.25
	Total	0.18	0.17	0.16	0.10	0.33	0.31	0.25

A, PB^0, uniform dielectric PB equation with DNA charges mapped to a grid and $\epsilon = 78.5$; B, PB^1, $\epsilon_{dna} = 78.5$, $\epsilon_{env} = 78.5$; C, PB^1, $\epsilon_{dna} = 2.0$, $\epsilon_{env} = 78.5$; D, PB^1, $\epsilon_{dna} = 2.0$, $\epsilon_{env} = 10, 25, 40, 60, 78.5$.

* R is the distance from the van der Waals surface of DNA to the center of the layer. The layer widths are 1.0, 2.0, 3.38, and 3.38 Å, respectively.

TABLE 2 Concentration (mol/liter) of 2-Å hard sphere counter-ions in the helical grooves of DNA (0.153 M PO_4) by radial layer

		No added salt				0.156 M added salt		
R (Å)*		A	B	C	D	B	C	D
3.0	Major groove	3.42	3.17	3.21	5.07	3.48	3.52	5.41
	Minor groove	0.00	0.00	0.00	0.00	0.00	0.00	0.00
	Elsewhere	1.23	1.31	1.27	1.44	1.63	1.60	1.82
	Total	1.88	1.86	1.84	2.53	2.18	2.17	2.89
5.69	Major groove	0.00	0.00	0.00	0.00	0.00	0.00	0.00
	Minor groove	0.00	0.00	0.00	0.00	0.00	0.00	0.00
	Elsewhere	0.54	0.47	0.48	0.35	0.66	0.67	0.55
	Total	0.54	0.47	0.48	0.35	0.66	0.67	0.55
9.07	Major groove	0.00	0.00	0.00	0.00	0.00	0.00	0.00
	Minor groove	0.00	0.00	0.00	0.00	0.00	0.00	0.00
	Elsewhere	0.22	0.21	0.21	0.15	0.37	0.37	0.31
	Total	0.22	0.21	0.21	0.15	0.37	0.37	0.31

A, PB^0, uniform dielectric PB equation with DNA charges mapped to a grid and $\epsilon = 78.5$; B, PB^1, $\epsilon_{dna} = 78.5$, $\epsilon_{env} = 78.5$; C, PB^1, $\epsilon_{dna} = 2.0$, $\epsilon_{env} = 78.5$; D, PB^1, $\epsilon_{dna} = 2.0$, $\epsilon_{env} = 10, 25, 40, 60, 78.5$.

* R is the distance from the van der Waals surface of DNA to the center of the layer. The layer widths are 1.0, 2.0, 3.38, and 3.38 Å, respectively.

using PB^1 was performed with a uniform dielectric coefficient of 78.5 for both the macro-ion and the environment and are tabulated in column B for comparison with the uniform dielectric calculation, PB^0, in column A. The discrepancies are fairly small and attributable to the finite size of the environmental shroud elements. In general, though, the agreement between PB^0 and PB^1 is good, indicating that the algorithms are functioning correctly.

The precision of the calculations depends on the size of the finite volume elements used to define the environmental shroud. Although this problem has been considered in earlier work (Klein and Pack, 1983) using the uniform dielectric coefficient algorithm, a set of calculations was done to ensure that the present dielectric boundary algorithm could be reliably implemented with a sufficiently fine grid with volume elements as shown in Fig. 2 (shroud 1). A grid was constructed for ions of sizes 1 and 4 Å for comparison with the results of calculations using shroud 1, which was for ions of 1, 2, and 4 Å radii. This grid (shroud 2) is displayed in Fig. 3. The difference between these two grids is that the second layer of shroud 2 (Fig. 3) precisely comprises the second and third layers of shroud 1 (Fig. 2).

Calculations of the distribution of 1 Å counter-ions neutralizing the polyion (no added salt) were done for both environmental shrouds, and the total amount of counter-ion charge in identical volumes (layers two and three of shroud 1 and layer two of shroud 2) was compared. For a PB^1 calculation in which the dielectric coefficient was assumed to

TABLE 3 Concentration (mol/liter) of 4-Å hard-sphere counter-ions in the helical grooves of DNA (0.153 M PO_4) by radial layer

		No added salt				0.161 M added salt		
R (Å)*		A	B	C	D	B	C	D
5.69	Major groove	0.00	0.00	0.00	0.00	0.00	0.00	0.00
	Minor groove	0.00	0.00	0.00	0.00	0.00	0.00	0.00
	Elsewhere	1.25	1.06	1.06	1.21	1.28	1.29	1.51
	Total	1.25	1.06	1.06	1.21	1.28	1.29	1.51
9.07	Major groove	0.00	0.00	0.00	0.00	0.00	0.00	0.00
	Minor groove	0.00	0.00	0.00	0.00	0.00	0.00	0.00
	Elsewhere	0.32	0.34	0.34	0.30	0.51	0.51	0.47
	Total	0.32	0.34	0.34	0.30	0.51	0.51	0.47

A, PB^0, uniform dielectric PB equation with DNA charges mapped to a grid and $\epsilon = 78.5$; B, PB^1, $\epsilon_{dna} = 78.5$, $\epsilon_{env} = 78.5$; C, PB^1, $\epsilon_{dna} = 2.0$, $\epsilon_{env} = 78.5$; D, PB^1, $\epsilon_{dna} = 2.0$, $\epsilon_{env} = 10, 25, 40, 60, 78.5$.

* R is the distance from the van der Waals surface of DNA to the center of the layer. The layer widths are 1.0, 2.0, 3.38, and 3.38 Å, respectively.

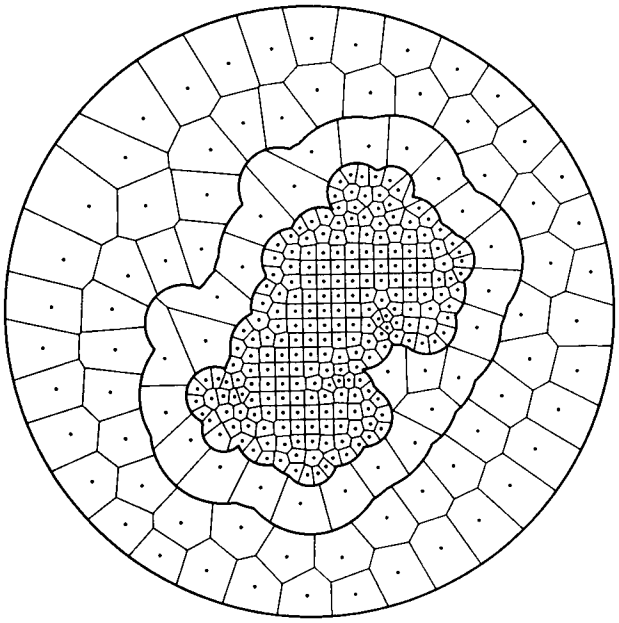

FIGURE 3 A gridded representation of DNA and shroud 2 analogous to Fig. 2. Layers 2 and 3 of shroud 1 (Fig. 2) have been combined into a single layer in this representation. The inner curved boundary excludes 1-Å spheres, and the outer curved boundary excludes 4-Å spheres.

be 78.5 everywhere, the amount of counter-ion charge was determined to be 0.458 and 0.464 for layers two and three of shroud 1, respectively, for a total of 0.922 compared to 0.903 for layer two of shroud 2, a difference of 2%. For a calculation in which a boundary was introduced by setting the dielectric coefficient of the elements within DNA to 2.0 and keeping that of the environment at 78.5, the amount of counter-ion charge in layers two and three of shroud 1 was calculated to be 0.605 and 0.375, respectively, for a total of 0.980. When the calculation was repeated using the coarser shroud 2, the calculated charge in layer two was 0.915, a discrepancy of about 7% attributable to the size of the finite elements. Similar calculations of the distribution of 4-Å ions indicate that the amount of counter-ion charge in layer four of shroud 1 is 0.764 compared with 0.762 in the identical layer three of shroud 2. Since the results to be discussed use the finer shroud 1, the greatest errors resulting for the smallest ion types at the DNA surface are likely to be less than 7%. For larger ions, these errors are expected to be substantially lower, since the major region in which errors occur are in the high electrostatic fields at the DNA surface from which larger ions are restricted.

Column C presents the results for a dielectric boundary calculation assuming the dielectric coefficient of DNA to be 2.0 and that of the solvent environment to be 78.5. As noted by Honig and co-workers (Jayaram et al., 1989), the potential in the minor groove is greatly altered by the presence of this dielectric boundary. The effect of the modified potential is highly localized, and the accumulation of counter-ions is significantly altered only in these restricted regions. In Table 1, the amount of charge due to 1-Å counter-ions in the minor groove is shown to be more than doubled when the dielectric boundary is introduced (compare columns B and C), implying that the potential near the surface of DNA (in the restricted volume of the minor groove) is much more negative when a dielectric boundary is introduced. This dielectric focusing due to the expulsion of the electric field from a material with a low dielectric coefficient is consistent with the work of others, as previously noted.

The extremely localized nature of the dielectric boundary focusing effect, as seen by its absence in the results of calculations on the 2-Å and 4-Å ions (Tables 2 and 3), shows it to be relatively less important for solvated counter-ions of moderate size. This is due to the inaccessibility of restricted crevices, in this case the minor groove, to ions with a radius equal to or larger than 2 Å. For comparison, the hydrodynamic radius of sodium in pure water is 1.83 Å and that of potassium is 1.25 Å (Adamson, 1979). The extent to which this very significant but highly localized enhancement of the electrostatic potential leads to an increase of counter-ion charge in the minor groove depends largely on the effective size of the counter-ions at the surface of DNA. If the waters of hydration of the counter-ion remain intact, the ions will be partially excluded from the minor groove. However, if the electrostatic field within the groove is sufficient to at least partially strip the ionic hydration shell and admit these ions, then dielectric focusing may be an important determinant of

the counter-ion concentration in the minor groove. Dynamic conformational fluctuations, transiently opening the groove, would be expected to alter the electrostatic field and allow access to certain restricted regions.

In order to determine the sensitivity of the dielectric boundary effect to the specific value of the dielectric coefficient, calculations giving the results presented in column D were performed. In these, it was assumed that the very strong electrostatic field at the macro-ion surface restricts the rotational freedom of nearby water molecules, thereby lowering the low-frequency dielectric coefficient (Booth, 1951a,b,c). In the first layer, extending 1 Å from the van der Waals surface of the DNA atoms, the dielectric coefficient was chosen to be 10. In the second, third, and fourth layers, with widths of 1, 2, and 3.38 Å, the dielectric coefficients were chosen to be 25, 40, and 60, respectively. Beyond 7.38 Å from the nucleic acid surface a bulk dielectric coefficient of 78.5 was assumed.

A comparison of columns D and C of Table 1 shows the effect exerted by variations of the dielectric coefficient close to the macro-ion surface. The lowering of the dielectric coefficient in the immediate vicinity of DNA drastically increases the concentration of small counter-ions in the first layer to which they have access. The major and minor groove concentrations of 1-Å ions increase from 4.9 and 8.5 M to 8.3 and 12.5 M, respectively, for the no-added-salt calculations, with similar increases for the 0.153 M added-salt case. The larger ions also are subject to the effects of this lower dielectric coefficient. Table 2 indicates that, although the introduction of the dielectric boundary had little effect on the counter-ion concentration (columns B and C), the lowering of the dielectric coefficient in the surface layers increases by a very significant amount the concentration in the first layer to which the 2-Å ions have access (columns D and C). Increases from 3.2 to 5.1 M and from 3.5 to 5.4 M are seen for the no-added-salt and 0.153 M added-salt cases, respectively. This effect of lower dielectric coefficient extends to the case of 4-Å ions reported in Table 3. The first layer to which these ions have access is centered at 5.69 Å and has a presumed dielectric coefficient of 60. This lower dielectric coefficient causes the net concentration in that layer to increase from 1.06 to 1.21 M and from 1.29 to 1.51 M for the two salt concentrations considered. This effect can most easily be attributed to the lower dielectric coefficient rather than any focusing of the field by the dielectric boundaries. These calculations emphasize the dependence of the results on the assumptions made regarding the properties of the system.

A stable surface concentration of counter-ions as a function of increasing salt concentration is a feature of the counter-ion condensation theory formulated by Manning (Manning, 1978). Since the present level of calculation is considerably more detailed than the line charge model used in the development of condensation theory, it is worth reconsidering where excess counter-ions accumulate as 1-1 monovalent salt is added. It should be restated that the calculations without added salt assumed that the DNA was confined to a cylindrical cell with a radius of 45 Å, which is equivalent to a PO_4 concentration of 0.153 M. The normalization condition of the PB equations assumes that the DNA charge is exactly neutralized by counter-ions that have access to the volume within that cylinder but is not occupied by DNA. The concentration of 1-Å counter-ions for the case with no added salt was 0.157 M. To simulate a concentration of 0.153 M added 1-1 monovalent salt, the required concentration is 0.310 M counter-ions with 0.153 M co-ions.

The addition of salt to the polyelectrolyte environment is predicted by PB (Wilson et al., 1980; Gueron and Weisbuch, 1980) and by MC (LeBret and Zimm, 1984; Murthy et al., 1985) to increase the surface concentration of counter-ion, an observation often cited as an indication of the failing of counter-ion condensation theory. Columns C (the calculation in which the dielectric coefficient abruptly increased from 2 to 78.5 at the macro-ion surface) in Table 1 show that there is an increased accumulation of about 16% (3.59 to 4.17 M) predicted in the surface layer when the number of 1-Å counter-ions in the environment is effectively doubled. For the variable dielectric model, in which the dielectric coefficient is increased in steps (columns D), the concentration is considerably greater, although the percentage increase is about 12%. Most of this accumulation is outside the grooves, where there is a 36% increase as compared to a 5% increase predicted within the major and minor grooves, suggesting that a saturation effect occurs. Columns D in Table 2 (2-Å ions) indicate that there is a 7% increase in the major groove and a 26% increase in the nongroove region of the closest layer to which 2-Å ions have access. There is a 25% increase in the surface layer for the 4-Å counter-ions, which are restricted from the grooves entirely (Table 3).

It has previously been suggested (Pack and Lamm, 1993) that although there is an increase in the amount of counter-ions present near the surface as the bulk concentration of counter-ions is increased, the amount of bound counter-ion charge per phosphate group remains constant. Table 4 presents the amount of bound counter-ion charge per phosphate group (the DNA charge fraction) calculated by the different approximations discussed above. Counter-ion condensation theory predicts a charge fraction of 0.76, somewhat larger than that predicted here by all of the calculations except the 1-Å hard sphere with a variable dielectric constant.

TABLE 4 Fraction of DNA charge neutralized by "bound" counter-ions

	B	C	D
1-Å hard-sphere ions			
No added salt	0.68	0.69	0.75
0.153 M added salt	0.65	0.67	0.77
2-Å hard-sphere ions			
No added salt	0.65	0.65	0.71
0.156 M added salt	0.65	0.62	0.70
4-Å hard-sphere ions			
No added salt	0.57	0.56	0.60
0.161 M added salt	0.48	0.48	0.56

B, PB[1], $\epsilon_{dna} = 78.5$, $\epsilon_{env} = 78.5$; C, PB[1], $\epsilon_{dna} = 2.0$, $\epsilon_{env} = 78.5$; D, PB[1], $\epsilon_{dna} = 2.0$, $\epsilon_{env} = 10, 25, 40, 60, 78.5$.

The charge fractions obtained here are quantitatively similar to those obtained using a uniform dielectric PB model (Pack and Lamm, 1993) and generally underestimate counter-ion condensation theory by about 10%. The implications of these results regarding the definition of counter-ion binding will be developed elsewhere.

It is remarkable that the number of counter-ions "bound" (by the $<-kT$ criterion) to DNA is not predicted by any of these models to increase as salt is added to the system. This stability may be compared to the increase in accumulation of surface counter-ions shown in Tables 1 to 3. This seemingly inconsistent behavior is imputed to the fact that the greater accumulation of surface counter-ion charge at higher concentrations of added salt (Tables 1 to 3) diminishes the electrostatic potential in all regions, thus contracting the volume in which the potential binds counter-ions.

CONCLUSIONS

The calculations presented here support previous conclusions (Jayaram et al., 1989) that the presence of a dielectric boundary significantly alters the electrostatic potential within the grooves of DNA. For small ions with effective radii of less than 2 Å, this magnified electrostatic potential may lead to an increase in concentration in the minor groove of DNA over that predicted using a uniform dielectric technique (Lamm and Pack, 1990). This is expected to be significant in the case of hydrogen ions, for example. For larger ions with restricted access to the grooves, this focusing of electric fields has little effect on their accumulation at the DNA surface. The results presented here underscore the importance of assigning an appropriate hard-sphere radius for solvated counter-ions.

Calculations assuming that the solvent dielectric coefficient near the DNA surface is diminished with respect to its bulk value suggest a very strong dependence of the results on the choice of parameters used to describe the system. Progressive variation of the dielectric coefficient from the bulk value of 78.5 beyond 7.38 Å from the DNA surface to a value of 10 in the layer at the first 1 Å from the surface results in a 70% increase of calculated counter-ion density, indicating that careful parameterization is required for a description of the environment as a dielectric continuum.

Hydrogen ions within the grooves reside on specific water molecules and have access to the same regions as individual waters hydrating the surface atoms of DNA. Previous calculations (Lamm and Pack, 1990) indicating that the p[H] ($= -\log_{10}[H^+]$) reaches about 4 in the minor groove were performed, assuming a uniform dielectric coefficient of 78.5. The calculations presented here suggest that $[H^+]$ may have been underestimated in that work.

Finally, the number of counter-ions in regions in which the electrostatic potential is more negative than $-kT$ is virtually identical for the no-added-salt calculation and the 0.153 M added-salt case. For most of the model systems this corresponds to a "bound fraction" of about 0.65. Because PB calculations generally underestimate the surface charge, this supports the conclusions of previous work (Pack et al., 1990) and agrees with the consequence of counter-ion condensation theory. The "bound fraction" of 0.76 obtained using the variable dielectric model with the 1-Å counter-ions is very intriguing and agrees quantitatively with Monte Carlo calculations of the association of hard-sphere counter-ions with cylindrical models of DNA in a continuum with a dielectric constant of 78.5 (Pack and Lamm, 1993; Lamm et al., 1993).

The helpful comments of the referees are appreciated.
This work was supported by grant GM29079 (G. R. P.) from the National Institutes of Health. Support from a Small Instrumentation Grant from the NIH (G. R. P.) is also gratefully acknowledged.

REFERENCES

Adamson, A. W. 1979. A Textbook of Physical Chemistry. Academic Press, New York.

Booth, F. 1951a. The dielectric constant of water and the saturation effect. *J. Chem. Phys.* 19:391–394.

Booth, F. 1951b. Errata: the dielectric constant of water and the saturation effect. *J. Chem. Phys.* 19:1327–1328.

Booth, F. 1951c. Erratum: the dielectric constant of water and the saturation effect. *J. Chem. Phys.* 19:1615.

Davis, M. E., and J. A. McCammon. 1991. Dielectric boundary smoothing in finite difference solutions of the Poisson equation: an approach to improve accuracy and convergence. *J. Comp. Chem.* 12: 909–912.

Gilson, M. K., A. Rashin, R. Fine, and B. Honig. 1985. On the calculation of electrostatic interactions in proteins. *J. Mol. Biol.* 183:503–516.

Gilson, M. K., M. E. Davis, B. A. Luty, and J. A. McCammon. 1993. Computation of electrostatic forces on solvated molecules using the Poisson-Boltzmann equation. *J. Phys. Chem.* 97:3591–3600.

Gueron, M., and G. Weisbuch. 1980. Polyelectrolyte theory 1. Counterion accumulation site binding and their insensitivity to polyelectrolyte shape in solutions containing finite salt concentrations. *Biopolymers.* 19:353–382.

Jayaram, B., K. A. Sharp, and B. Honig. 1989. The electrostatic potential of B-DNA. *Biopolymers* 28:975–993.

Klapper, I., R. Hagstrom, R. Fine, K. Sharp, and B. Honig. 1986. Focusing of electric fields in the active site of Cu-Zn superoxide dismutase: effects of ionic strength and amino acid modification. *Proteins Struct. Funct. Genet.* 1:47–59.

Klein, B., and G. R. Pack. 1983. Calculations of the spatial distribution of charge density in the environment of DNA. *Biopolymers.* 22:2331–2352.

Lamm, G., and G. R. Pack. 1990. Acidic domains around nucleic acids. *Proc. Natl. Acad. Sci. USA.* 87:9033–9036.

Lamm, G., L. Wong, and G. R. Pack. 1993. Monte Carlo and Poisson-Boltzmann calculations of the fraction of counterions bound to DNA. *Biopolymers.* In press.

LeBret, M., and B. H. Zimm. 1984. Monte Carlo determination of the distribution of ions about a cylindrical polyelectrolyte. *Biopolymers.* 23: 271–285.

Manning, G. S. 1978. The molecular theory of polyelectrolyte solutions with applications to the electrostatic properties of polynucleotides. *Q. Rev. Biophys.* 2:179–246.

Murthy, C. S., R. J. Bacquet, and P. J. Rossky. 1985. Ionic distributions near polyelectrolytes. A comparison of theoretical approaches. *J. Phys. Chem.* 89:701–710.

Pack, G. R., and B. Klein. 1984. Generalized Poisson-Boltzmann calculation of the distribution of electrolyte ions around the B- and Z-conformers of DNA. *Biopolymers.* 23:2801–2823.

Pack, George R., and G. Lamm. 1993. Counterion condensation theory revisited: limits on its applicability. *Int. J. Quantum Chem. Quantum Biol. Symp.* (in press).

Pack, G. R., L. Wong, and C. V. Prasad. 1986a. Counterion distribution around DNA. *Nucleic Acids Res.* 14:1479–1493, 5574.

Pack, G. R., C. V. Prasad, J. S. Salafsky, and L. Wong. 1986b. Calculations on the effect of methylation on the electrostatic stability of the B- and Z-conformers of DNA. *Biopolymers.* 25:1697–1715.

Pack, G. R., G. Lamm, L. Wong, and D. Clifton. 1990. The structure of the electrolyte environment of DNA. *In* Theoretical Biochemistry and Molecular Biophysics. D. L. Beveridge and R. Lavery, editors. Adenine Press, New York. 237–246.

Rogers, N. K., G. R. Moore, and M. J. E. Sternberg. 1985. Electrostatic interactions in globular proteins: calculation of the pH dependence of the redox potential of cytochrome c_{551}. *J. Mol. Biol.* 182:613–616.

Wachspress, E. L. 1966. Iterative Solution of Elliptic Systems. Prentice Hall, Englewood Cliffs, NJ.

Warwicker, J. 1986. Continuum dielectric modelling of the protein-solvent system and calculation of the long-range electrostatic field of the enzyme phosphoglycerate mutase. *J. Theor. Biol.* 121:199–210.

Warwicker, J., and H. C. Watson. 1982. Calculation of the electric potential in the active site cleft due to α-helical dipoles. *J. Mol. Biol.* 157:671–679.

Warwicker, J., D. Ollis, F. M. Richards, and T. A. Steitz. 1985. Electrostatic field of the large fragment of *Escherichia coli* DNA polymerase I. *J. Mol. Biol.* 186:645–649.

Wilson, R. W., D. C. Rau, and V. A. Bloomfield. 1980. Comparison of polyelectrolyte theories of the binding of cations to DNA. *Biophys. J.* 30:317–326.

You, T. J., and S. C. Harvey. 1992. Finite element approach to the electrostatics of macromolecules with arbitrary geometries. *J. Comp. Chem.* 14:484–501.

Zauhar, R. J., and R. S. Morgan. 1985. A new method for computing the macromolecular electric potential. *J. Mol. Biol.* 186:815–820.